IOPscience iopscience.iop.org

Home Search Collections Journals About Contact us My IOPscience

Low temperature synthesized Sn doped indium oxide nanowires

This content has been downloaded from IOPscience. Please scroll down to see the full text.

2005 Nanotechnology 16 451

(http://iopscience.iop.org/0957-4484/16/4/021)

View the table of contents for this issue, or go to the journal homepage for more

Download details:

IP Address: 140.113.38.11
This content was downloaded on 26/04/2014 at 12:24

Please note that terms and conditions apply.

Nanotechnology **16** (2005) 451–457 doi:10.1088/0957-4484/16/4/021

Low temperature synthesized Sn doped indium oxide nanowires

Seu Yi Li[1], Chia Ying Lee[2], Pang Lin[1] and Tseung Yuen Tseng[2,3]

[1] Institute and Department of Materials Science and Engineering, National Chiao Tung University, Hsinchu 30049, Taiwan
[2] Department of Electronics Engineering and Institute of Electronics, National Chiao Tung University, Hsinchu 30050, Taiwan

E-mail: tseng@cc.nctu.edu.tw

Received 2 October 2004, in final form 14 December 2004
Published 11 February 2005
Online at stacks.iop.org/Nano/16/451

Abstract
Selective, well controlled and directionally grown Sn doped In_2O_3 nanowires (In_2O_3: Sn nanowires, SIO NWs) were synthesized at a low fabrication temperature (∼770 °C) through a vapour–liquid–solid (VLS) process under a precise carrier gas flow. The majority of the SIO NWs are grown along [222], with [400] and [440] as minority forming directions, which implies a nearly epitaxial crystal structure. There are fewer physical defects, such as line or planar defects and contaminations, in the SIO NWs than in pure In_2O_3 nanowires seen through high resolution transmission electron microscopy (HR-TEM) observations. The spectrum of photoluminescence (PL) emission indicates a stable strong blue light peak located at ∼440 nm with an excited wavelength of 275 nm at room temperature. The Sn dopant in the SIO NWs can enhance the conductivity of the nanowires leading to the lowering of the turn-on electric-field to 0.66 V μm^{-1} under a current density of up to 1.0 mA cm^{-2} based on their field emission characteristics. Furthermore, the field emission enhancement coefficient, β, is also increased to 1.48×10^5, which is very close to the carbon nanotube, (CNT) level. SIO NWs fabricated by a VLS process offer a potential application in flat panel displays as demonstrated in this study.

1. Introduction

Recently, much progress in the synthesis of metal oxide nanowires (especially II–VI semiconductor materials) has been driven by the requirement to explain the novel physical and optical properties of one and two dimensional nanostructures such as nanorods, nanobelts, or nanowires (NWs), and nanofilms. Furthermore, their potential applications in constructing nanoscale electronic and optoelectronic devices are equally subjected to more attention. The wide band gap transparent conductor material indium oxide (In_2O_3; IO) has a direct band gap of ∼3.6 eV and an indirect band gap of ∼2.6 eV, which has been studied to be used in microelectronic fields [1]. However, previous research has mainly focused on the applications of films or particles [2, 3]. The investigation of nanowires (1D nanostructure) of IO is still quite limited [4, 5]. The fabrication processes that have been reported for the synthesis of IO NWs are thermal evaporation and electrodeposition and oxidation. On the basis of our previous study [6, 7], the vapour–liquid–solid (VLS) process is able to offer improved stability and large area growth of nanowires on Si substrates under easily tunable controlled conditions. In this work, the VLS method is employed to synthesize IO NWs, and their field emission properties are studied. In order to promote the electronic conductivity and lower the turn-on electric field for the field emission (FE) characteristic, SnO_2 powders were added into the pure IO source powders in the VLS process so that that would lead to the diffusion of Sn into the IO NWs. The morphology and crystal structure of the Sn doped IO NWs (SIO NWs) are also investigated.

2. Experimental details

A Radio Corporation of America (RCA) cleaning method was used to clean a p-type Si(100) substrate. This process can

[3] Author to whom any correspondence should be addressed.

remove the native oxide (∼20 Å) from the surface of the Si substrate. After the cleaning procedure, a 70 Å thick Au film with a diameter of 100 μm was formed on the Si(100) substrate by rf-sputtering (13.56 MHz) under 10 mTorr Ar atmosphere at a power level of 30 W for 15 s and then patterned by the shadow mask process. This Au film acts as a catalyst for SIO NWs synthesized through a precise carrier gas flow-controlled VLS process and the control of the growth region of the nanowires.

The source material for SIO NWs was a mixture of IO (99.998%), SnO_2 (99.98%), and graphite (99.98%) powders at a molar ratio of 0.9:0.1:1.0. The mixed powders were put on the quartz boat in front of the Au/Si substrate loaded in a horizontal alumina tube furnace. The SIO NWs were synthesized by the VLS process with temperatures varying from 770 to 950 °C. The furnace was heated at a rate of 150 °C min^{-1} under a gas flow rate of high purity N_2 (99.998%) varying from 20.0 to 100.0 cm^3 s^{-1}. The optimized gas flowing rate used in our study was 60.0 cm^3 s^{-1}. On the basis of our previous study [7], the carrier gas being controlled to nearly laminar flow mode in the horizontal furnace is able to be helpful in the vertical growth of the nanowires. The crystal structure of the nanowires was studied by x-ray diffraction (XRD, MAC Science, MXP18, Japan). The morphology and microstructures of the SIO NWs were analysed by field emission scanning electron microscopy (FE-SEM, Hitachi S-4700I, Japan) and high resolution transmission electron microscopy (HRTEM, Philips tecani-20, USA). The chemical composition of the nanowires was characterized by x-ray photoelectron spectroscopy (XPS, VG Scientific Microlab 250, UK). A photoluminescence analyser (PL, Hitachi F-4500, Japan) with Xe lamp as an excitation source (275 nm) was used for the optical studies at room temperature. A high voltage–current instrument, Keithley 237, was used to analyse the FE characteristic of the SIO NWs. A tungsten tip probe and a controllable sample stage were all loaded in a high vacuum chamber kept under 10^{-8} Torr in the FE measurement.

3. Results and discussion

The XRD patterns shown in figure 1(a) indicate the influence of growth temperature on the crystallinity of the SIO NWs. When the growth temperature is decreased from 900 to 770 °C, the intensities of the XRD peaks such as (222), (400), and (440) of the SIO NWs [8] become stronger. Based on SEM observations (not shown here), the nanowire density, which may also affect the peak height, does not show any difference among SIO NWs grown at different temperatures. The relation of full-width at half-maximum (FWHM) versus growth temperature is shown in figure 1(b). The FWHM value decreases with a decrease in synthesis temperature from 900 to 770 °C. When the synthesis temperature is lowered to 750 °C or below, the SIO NWs were unable to be successfully grown at those temperatures. That means that if the growth temperature is too low (≦750 °C), a suitable amount of vapour of In or Sn is hardly formed, and as a result it is difficult to carry the VLS process out. On the other hand, such a low temperature does not provide enough energy to crystallize the SIO NWs. It is shown in figure 1(a) that a very weak diffraction peak appears for SIO NWs grown at 750 °C. When the synthesis temperature is 770 °C, the intensity of the (222) peak is the highest, and the FWHM value of ∼0.14° is the smallest, implying that this temperature is more suitable for the growth of SIO NWs with a good cubic crystal structure. At higher growth temperature such as 900 °C or above, the lattice structure becomes poor which may be due to the Sn^{4+} being vaporized and being taken away from the system through the carrier gas, leading to the intensity of the (222) peak becoming weak. The growth

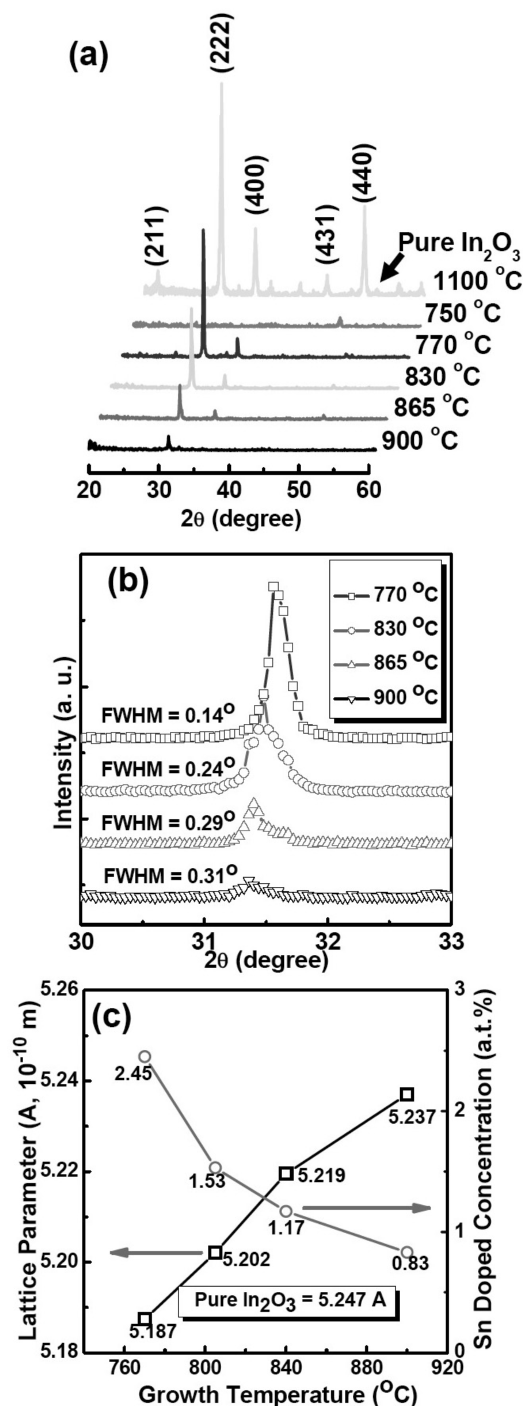

Figure 1. (a) XRD patterns of the SIO NWs at different synthesis temperatures from 770 to 900 °C, (b) effect of growth temperature on the FWHM value of the SIO NWs, and (c) the lattice parameter and atomic weight percentage of Sn doping at different synthesis temperatures.

temperatures reported in the previous papers of IO NWs were usually about ∼900–1100 °C [9, 10]. Obviously, the Sn dopant could effectively decrease the growth temperature of the SIO NWs through the VLS process. In the VLS process, the mixed metal oxide powders, IO and SnO_2, are reduced to metal droplets by graphite at a high temperature, typically at ∼1100 °C for pure IO. The melting point of the In–Sn alloy is ∼393 °C while the Sn content is less 10 wt% [11]. The melting point of this alloy is lower than that of pure In. Therefore, the Sn dopant would effectively decrease the temperature for the droplet to form, which is helpful to decrease the synthesis temperature of the SIO NWs. Furthermore, when the synthesis temperature decreased from 900 to 770 °C, the (222) peak of the SIO NWs was shifted towards higher 2θ value, which is closer to 32° as shown in figure 1(a). The lattice parameter of SIO NWs versus the growth temperature is shown in the figure 1(c) which indicates the change in the a parameter calculated from the angle shift of the (222) peak of the SIO NWs. The ionic radii of In and Sn are 1.56 and 1.45 Å, respectively [12]. The shift in the diffraction angle of the XRD patterns of nanowires could be due to the diffusion of Sn into the IO lattice sites that leads to the shrinkage of lattice parameters of pure IO. On the other hand, additions of SnO_2 to IO form a solid solution with cubic structure in which Sn^{4+} are substituted for In^{3+}, resulting in the formation of an In vacancy to keep the cation–anion site relationship of 2:3.

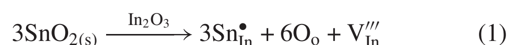

$$3SnO_{2(s)} \xrightarrow{In_2O_3} 3Sn^{\bullet}_{In} + 6O_o + V'''_{In} \quad (1)$$

where $Sn^{\bullet}_{In}$ means Sn substituted for In^{3+} in IO, O_o denotes O at the same oxygen site, and V'''_{In} means a vacancy at a In^{3+} site in the lattice of the SIO NWs. The amount of Sn in the nanowires shown in figure 1(c) which was measured by EDS analysis is decreased with the synthesis temperature increasing from 770 to 900 °C, which is manifested as a less-shifted diffraction angle of the (222) peak.

The selective growth of the SIO NWs in the Au catalyst film pattern with a diameter of about 100 μm is shown in figure 2(a). The VLS growth process was carried out at a temperature of 770 °C for 3.0 h under an N_2 carrier gas flow rate of 60.0 $cm^3\ min^{-1}$. Figure 2(b) shows the FE–SEM images of the boxed region in figure 2(a). The clear demarcation demonstrates that only the area defined by the Au catalyst film promotes the synthesis of SIO NWs by the VLS process. Furthermore, the more vertical growth direction SIO NWs are found at the centre of the location of the Au pattern as shown in figure 2(c). The SIO NWs at the edge of the Au pattern (see figure 2(d)) have random growth direction. The SIO NWs are about 10 μm long and the average diameter is about 80 nm. The sidewall of the nanowires is very smooth and the geometry of these SIO NWs is uniform. This result is also proved by HR-TEM analysis in a later section. According to the high resolution SEM observation, there are some Au catalyst droplets that still adhere on the front of the SIO NWs tips.

A selected area electron diffraction (SAED) pattern of the SIO NWs grown at 770 °C along the [001] axis is shown in figure 3(a). The indexed diffraction patterns corresponding to (200) and (220) indicate that the SIO NWs have a cubic crystalline structure. The clear spots also prove that the SIO NWs are single crystalline structures. After a d-spacing

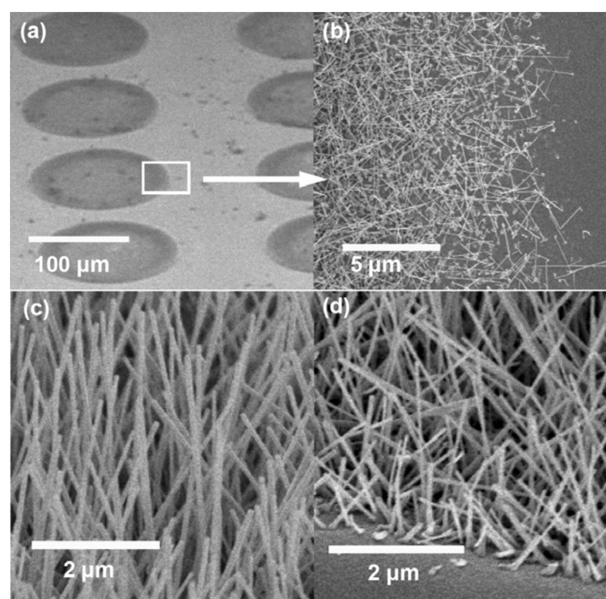

Figure 2. FE–SEM images of the SIO NWs: (a) large area of the selective synthesis process of SIO NWs, (b) a zoom in photograph of the edge of the 100 μm diameter metal mask for selective growth, (c) 45° tilted view for 10 μm length and ∼80 nm diameter of the SIO NWs at the central region and (d) the outside region near the circle of SIO NW growth.

calculation, the lattice parameter of the SIO NWs is ∼5.19 Å along the a-axis, which is consistent with the analysis results of the XRD as shown in figure 1(c). The bright view image given in figure 3(b) shows the geometry and morphology of the SIO NWs. The sidewall of the nanowires is very smooth, which agrees with the SEM result. Generally, there is some metal tip remaining, which is shown in this image (figure 3(b)). The lattice fringes shown in the HR-TEM photograph of the SIO NWs in figure 3(c) correspond to a cubic structure. The clear contrast of the lattice image indicates the arrangement of In and O in the nanowires. The lattice distance between each fringe is ∼5.19 Å along the [200] direction. Figures 3(d) and (e) depict the computer simulation analysis (Gaton, Inc. DigitalMicrograph^{TM}3) results of the SIO NWs. Figure 3(d) is the modified pattern of the SAED obtained from the transformation of figure 3(c) using the fast Fourier transform (FFT) method. The indexed spots in this pattern are consistent with those in figure 3(a), which again proves that the fabricated SIO NWs have a well-defined cubic crystalline structure. The high-resolution image shown in figure 3(e) is obtained by the inverse fast Fourier transformation (IFFT) of the SAED pattern of figure 3(a) after removing background noise. The clear lattice fringes along the c-axis in figure 3(e) are consistent with those in figure 3(c). We can obviously produce clearer atomic images of the NWs (figures 3(d) and (e)) through the application of simulation tools. It is demonstrated by figure 3 that the VLS process can be employed to fabricate high-quality SIO NWs that have well-defined cubic crystalline structure and fewer lattice defects than IO NWs reported in previous studies [4, 5].

The high-resolution EDS spectra (figures 4) indicate the constituent elements and the chemical composition of the SIO NWs grown at 770 °C. There are three clear peaks of In that

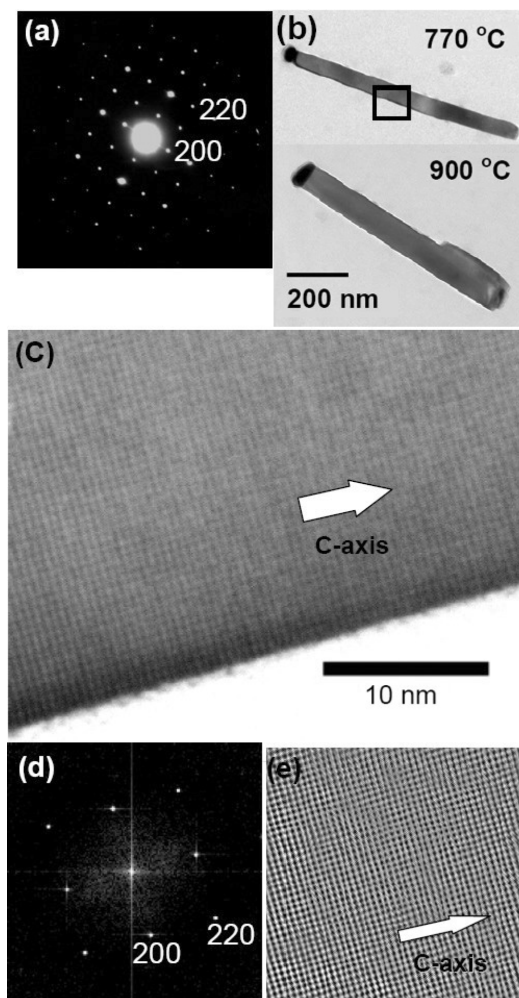

Figure 3. TEM photograph of a single crystalline SIO NW: (a) indexed SAED diffraction pattern, (b) bright view of the SIO NW, (c) HR–TEM image showing the lattice fringes, (d) simulated SAED pattern that is consistent with (a), (e) IFFT image for (c).

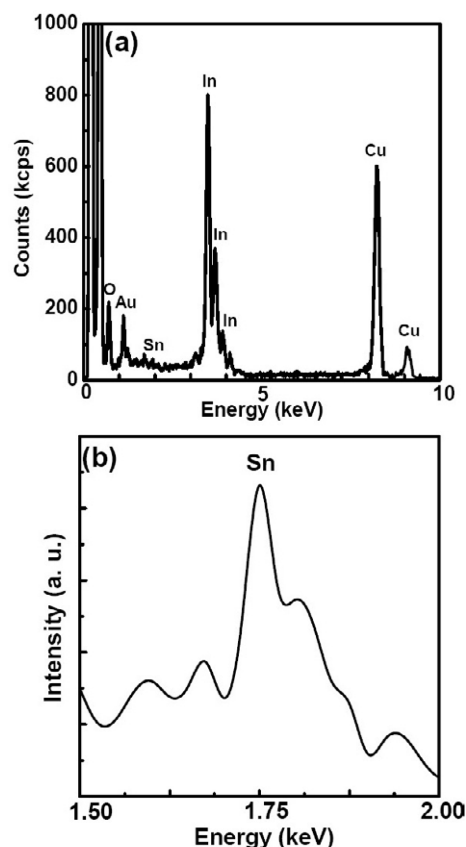

Figure 4. (a) EDS spectra indicating the elemental In, O, and Sn distributions in the SIO NWs, (b) EDS spectrum of Sn peaks of the SIO NWs grown at 770 °C.

have been easily detected and some other elements have also been found. The clear In and O peaks located at ∼3.5 keV (main peak) and ∼0.65 keV, respectively can indicate the composition of the nanowires. Through the semi-quantitative analysis, the chemical composition of In/O of the SIO NWs is about 0.38/0.59 by atomic weight per cent ratio. Furthermore, according to the EDS spectrum as shown in figure 4(b), the weak peak located at ∼1.75 keV is identified as Sn. The amount of Sn dopant is ∼2.45 at.% from a quantitative analysis of this spectrum. That means that the VLS process can offer good control for the chemical composition for fabricated SIO NWs. On the other hand, the Cu signal comes from the TEM copper grid holder. The Au signal has been detected from the tip in front of the SIO NWs. This result demonstrates that the Au catalyst remains throughout the VLS process.

The XPS spectra shown in figure 5(a) depict the full region scanned from 0 to 1200 eV with respect to two different areas of the same Si substrate in which one is the spectrum (1) and the other is the bare Si surface without patterning SIO NWs in the Au patterned surface (spectrum (2)). When the electron beam focuses on the patterned surface in which the SIO NWs exist, it indicates that some elements, such as C, O, Si, In_{3p}, In_{3d}, In_{4p}, In_{4d} and Sn_{3d} can be clearly detected in this area, as observed in XPS spectrum (1) of figure 5(a). This result further proves the selective growth process of the SIO NWs in our experiment. The high-resolution scanned information provided in figures 5(b)–(d) is for the separated analysis of elements, O, In, and Sn, respectively. The high-resolution XPS spectrum of the O_{1s} signal (figure 5(b)) indicates that the binding energy is ∼529.6 eV, which is consistent with that of O_{1s} in In_2O_3. Furthermore, another O_{1s} peak, at 533.5 eV, is indicating that less Sn bonded with O, while Sn^{4+} diffuses into the nanowires. Figure 5(c) shows the peaks of ∼452.3 eV for $3d_{3/2}$ and ∼445.6 eV for $3d_{5/2}$ of In, respectively. The $3d_{3/2}$ and $3d_{5/2}$ in figure 5(d) are marked as ∼495.4 and 486.3 eV that represent the Sn dopant diffused into those nanowires through the fabricated process. For different growth temperatures from 770 to 900 °C, the amount of Sn dopant decreases from 2.45 to 0.83 atomic weight per cent with increasing synthesis temperature, as shown in figure 1(b). This spectral information of 770 °C synthesized materials was calculated by an analytical process. The atomic weight percentages of In, Sn and O in nanowires grown at 770 °C are ∼38.6%, ∼2.43%, and ∼58.8%, respectively, based on the calculation from the XPS spectra, which are in good agreement with those obtained from the EDS measurements.

The room temperature photoluminescence (PL) spectra of the SIO NWs grown at various temperatures from 770 to 900 °C are shown in figure 6. It is well known that bulk In_2O_3 can just

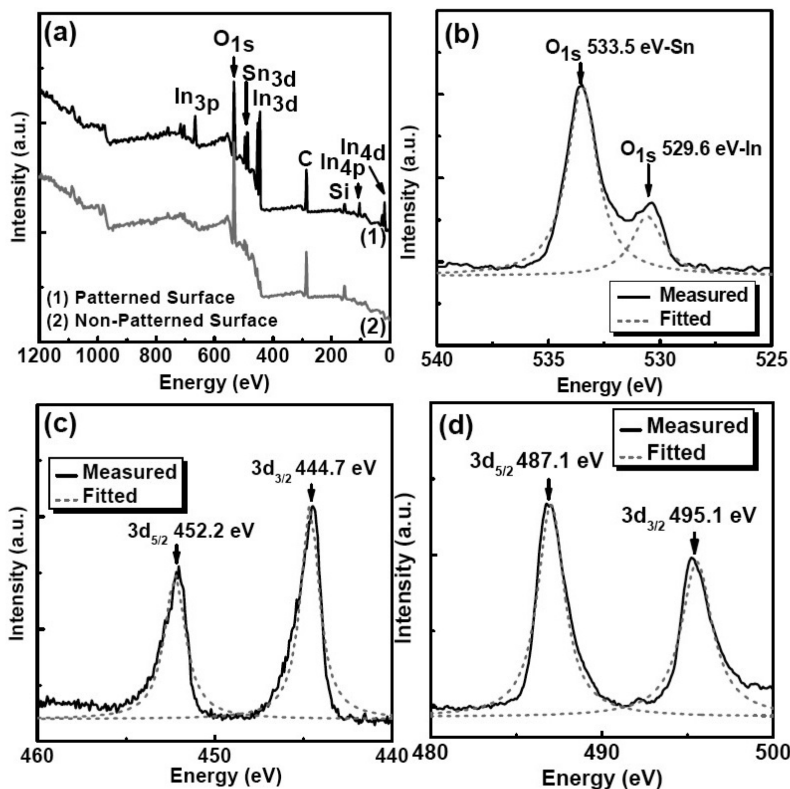

Figure 5. XPS spectra of the SIO NWs: (a) fully scanned from 0 to 1200 eV, (b) high resolution selective spectrum of O, (c) high resolution selective spectrum of In, and (d) high resolution selective spectrum of Sn, respectively.

emit very weak light at room temperature. However, a stronger and sharper PL emission spectrum from the SIO NWs is shown in the present study. Under the excited wavelength of 260 nm of an Xe lamp, a broadened optical emission spectrum located at ∼400–460 nm has been found, in which four distinct peaks can be easily observed: one is at ∼425 nm which originated from the Si(100) substrate, while the others excited by the SIO NWs are located at 416, 440, and ∼446 nm. Based on previous reports [9, 10], the strong PL emission of the IO NWs was located at ∼416 nm. The strongest PL emission peak of the SIO NWs in the present study is located at 440 nm instead of 416 nm (figure 6), which reveals an optical band gap of ∼2.82 eV. As the Sn is doped into IO NWs, the main emitted peak shifts toward the longer wavelength, indicating that the Sn addition would create new separated band gap levels (E_g) of SIO NWs. The difference in energy between these levels is smaller than that in IO NWs, which can result in longer wavelength emission. Such E_g lowering can be attributed to the formation of localized band edge states due to charge exchange and structural relaxation, and is proportional to the orbital energy and the size difference between atoms of the elements. The blue emission located at 440 nm can be explained by the following step. An electron in the donor level is captured by a hole on an acceptor (V_{In} and V_{Sn}) which becomes a radiative recombination centre to emit blue light; that is, the creation of vacancies due to the addition of Sn is the cause of the mean emission of the SIO NWs at 440 nm instead of 416 nm. Furthermore, higher fabrication temperatures ranging from ∼800 to 900 °C can prompt the main emission peak to shift to longer wavelength (440–446 nm) because at the higher temperature process, metal vacancies such as V_{In} or V_{Sn} would increase speedily and will cause longer wavelength to be emitted. The appearance of an upper tail at 475 nm of the PL spectrum (figure 6) indicates the ionized oxygen vacancies, $V_O^{\bullet}$ or $V_O^{\bullet\bullet}$, that contribute to some new energy levels in the band gap of the SIO NWs.

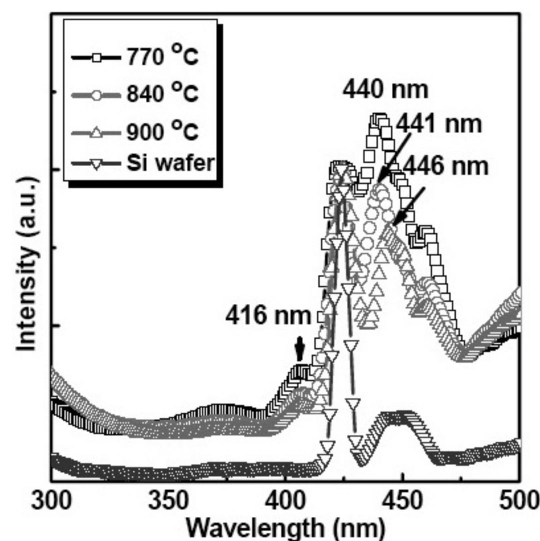

Figure 6. Emission spectra of the SIO NWs using 275 nm incident Xe lamp at room temperature (298 K).

The field emission (FE) characteristics of the SIO NWs grown at 770 and 900 °C are shown in figure 7, indicating that their I–V characteristics follow a Fowler–Nordheim (FN) behaviour. The FN plot in the inset of figure 7 where

Table 1. The field emission characteristics of carbon nanotubes (CNTs) and oxide NWs with and without Sn doping. (Note: E_{to} is the turn-on electric field, J_{to} the turn-on current density, β the field emission enhancement factor, R_s the turn-on series resistance, and T_{growth} the synthesis temperature.)

	E_{to} (V μm^{-1})	J_{to} (mA cm^{-2})	β	R_s (kΩ)	T_{growth} (°C)	Reference
CNTs	1.4	10–30	10 600	N/A	500	[13]
CNTs	1.5–4.5	0.01–0.1	1000–3000	N/A	N/A	[14]
CNTs	4.0	2.0	1500	N/A	750	[18]
ZnO NWs	0.83	1.0	7180	85.43	900	[15]
ZnO NWs	0.7	1.0	40 000	N/A	1100	[16]
SZO NWs	0.15	1.0	445 000	24.52	820	[19]
IO	2.7	10^{-3}	1600	N/A	950	[20]
SIO NWs	0.68	1.0	148 000	18.3	770	Present work

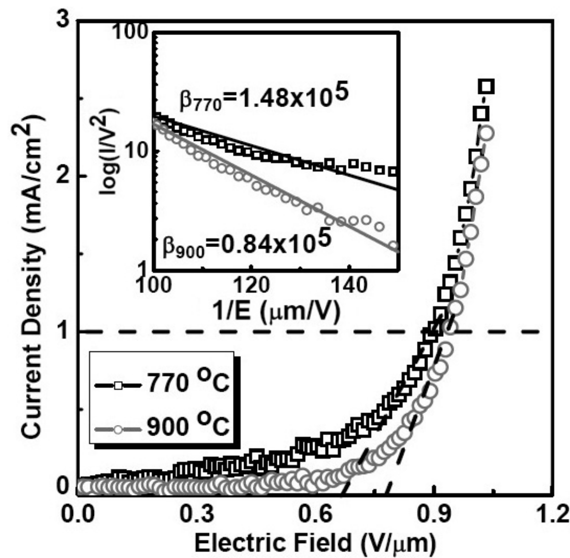

Figure 7. Field emission characteristic of the SIO NWs; the inset is the FN plot that is calculated from the field emission enhancement coefficient.

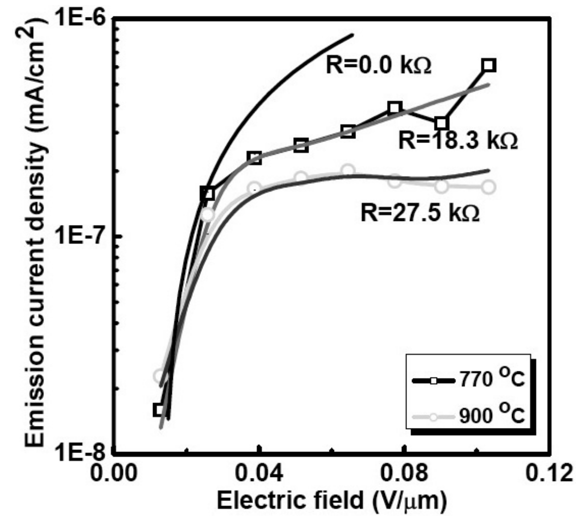

Figure 8. Emission current density versus lower electric field of the SIO NWs grown at different temperatures, 770 and 900 °C.

$\log(I^2/V)$ is plotted as a function of $1/E$ are characterized by two constant slopes for two different synthesis temperatures. The turn-on electric field of SIO NWs grown at 770 °C is ~0.66 V μm^{-1} at 1.0 mA cm^{-2} and its field emission enhancement coefficient, β, is 1.48×10^5. On the other hand, as the growth temperature is raised to 900 °C, the turn-on electric field and the β value are ~0.78 V μm^{-1} and 0.84×10^5, respectively. Such an increase in the turn-on electric field and decrease in the β value may be attributed to poor crystallinity of the SIO NWs grown at higher temperature. Furthermore, in comparison with other nanowires such as CNTs [13, 14, 18], ZnO NWs [15, 16, 19] and IO [20] NWs listed in table 1, our SIO NWs have lower turn-on electric field and larger enhancement factor, β, than IO [20]. This difference can be attributed to the Sn being doped into the IO NWs, which results in the increase of the conductivity and consequently leads to lowering the turn-on electric field and enhancing the β value of the NWs.

The resistances of the SIO NWs grown at different temperatures are shown in figure 8. The saturation of the field emission current occurs in SIO NWs grown at 770 and 900 °C. Each SIO NW has its own highest resistance at below the turn-on electric-field. The drop of voltage across such a resistor would decrease the effective applied voltage, and therefore cause a flattening of the characteristics to occur [17]. After fitting to the low emission current part of the measured data, the resistances corresponding to SIO NWs grown at 770 and 900 °C are 18.3 and 27.5 kΩ, respectively. The decrease in resistance is proportional to the increase in Sn dopant concentration, which means the lower the growth temperature the more the amount of Sn dopant diffusion. The lower resistance occurring in SIO NWs grown at 770 °C which have a larger amount of Sn dopant may be attributed to the Sn-enhanced electron density and higher concentration of In vacancies (equation (1)). Furthermore, the field-adjustment factor, α, is an index to determine the ability to enhance the local field from the field emission tips. In this study, the α-values for 770 and 900 °C grown nanowires are 2.34×10^{-4} and 2.29×10^{-4}, respectively, indicating that the SIO NWs synthesized at 770 °C have larger α value than those grown at 900 °C. In fact, the better crystal structure of SIO NWs grown at 770 °C effectively develops the α-value because less impurity and fewer defects will help the free electron emission mechanism under the low electric field. This result can also be explained that the more vertical the growth of the tips of the SIO NWs, the better the ability to enhance local electric field.

On the basis of the field emission characteristics of oxide NWs and CNTs displayed in table 1, the turn-on electric field is effectively decreased by the Sn dopant for those NWs. The turn-on electric field is decreased four times and the

β-value is enhanced two orders due to the Sn being doped into IO NWs. Meanwhile, with the same Sn doping level (~2.45 at.%), the SIO NWs have lower series resistance than the Sn doped ZnO (SZO) NWs that would enhance the stability of the emission current. Besides, the SIO NWs have lower synthesis temperatures than the SZO NWs which have a better opportunity to easily integrate into the semiconductor technology. As for the comparison between CNTs and oxide NWs, most oxide NWs have lower turn-on electric field than CNTs, but CNTs have lower synthesis temperatures as listed in table 1.

4. Conclusions

In summary, SIO NWs are successfully fabricated by the VLS process at a low temperature of 770 °C. The Sn dopant can effectively decrease the synthesis temperature of SIO NWs from ~1100 to 770 °C. The geometry and morphology (80 nm diameter and ~10 μm length) of the SIO NWs are perfect without much contamination. On the basis of the fabrication process, these nanowires have a well-defined cubic crystal structure and fewer defects or dislocations. On the other hand, the SIO NWs emitted a strong blue light band at ~445 nm at room temperature by using a Xe lamp (275 nm) as the excitation source. Furthermore, the Sn dopant could also shift the main emission of the SIO NWs to a shorter wavelength. Therefore, the synthesis of SIO NWs would possess technological promise for manipulating the nano-optical properties, which is important in nanoscale optoelectronic applications. The field emission measurements indicated the low turn-on electric field of 0.66 V μm^{-1} at a current density of 1.0 mA cm^{-2}. The low temperature fabricated (~770 °C) SIO NWs exhibited a higher field emission area factor of about 1.48×10^5 and larger field adjustment factor of 2.34×10^{-4} than those values of the 900 °C fabricated nanowires, which is due to the Sn dopant that remained more in the nanowires when fabricated at 770 °C. The amount of Sn dopant added in the SIO NWs is ~2.45 at.%, which lowers the resistance and increases the conductivity, respectively. Using these structurally controlled Sn doped SIO NWs, more interesting physical and chemical properties can be studied. Therefore, the vertically and selectively grown SIO NW array is a good candidate for future flat panel display applications.

Acknowledgment

This work was supported by the National Science Council of R.O.C. under contract number NSC 93-2216-E-009-024.

References

[1] Zhang D H, Li C, Liu X L, Han S, Tang T and Zhou C W 2003 *Appl. Phys. Lett.* **83** 1845
[2] Luo J K and Thomas H 1993 *Appl. Phys. Lett.* **62** 705
[3] Shigesato Y, Takaki S and Haranoh T 1992 *J. Appl. Phys.* **71** 3356
[4] Zheng M J, Zhang L D, Li G H, Zhang X Y and Wang X F 2001 *Appl. Phys. Lett.* **79** 839
[5] Chun H J, Choi Y S, Bae S Y, Choi H C and Park J 2004 *Appl. Phys. Lett.* **85** 461
[6] Li S Y, Lee C Y and Tseng T Y 2003 *J. Cryst. Growth* **247** 357
[7] Li S Y, Lin P, Lee C Y and Tseng T Y 2004 *J. Mater. Sci.* **15** 505
[8] *ICDD, International Center for Diffraction Data, JCPDS-ICDD,* 2000
[9] Chun H J, Choi Y S, Bae S Y, Choi H C and Park J 2004 *Appl. Phys. Lett.* **85** 461
[10] Edwards D D, Folkins P E and Mason T O 1997 *J. Am. Chem. Soc.* **80** 253
[11] Ezaki H, Nambu T, Ninomiya R, Nakahara Y, Wang C Q and Morinaga M 2002 *J. Mater. Sci.* **13** 169
[12] Stwertka A and Stwertka E 1999 *WebElements^{TM} Periodic Table* professional edition (USA: WebElements Book Store)
[13] Umnov A G and Mordkovich V Z 2001 *Appl. Phys.* A **73** 301
[14] Bonard J M, Salvetat J P, Stöckli T, de Heer W A, Forró L and Châtelain A 1998 *Appl. Phys. Lett.* **73** 918
[15] Li S Y, Lin P, Lee C Y and Tseng T Y 2004 *J. Appl. Phys.* **95** 3711
[16] Jo S H, Banerjee D and Ren Z F 2004 *Appl. Phys. Lett.* **85** 1407
[17] Bonard J M, Klinke C, Dean K A and Coll B F 2003 *Phys. Rev.* B **67** 115406
[18] Wong Y M, Wei S, Kang W P, Davidson J L, Hofmeister W, Huang J H and Cui Y 2004 *Diamond Relat. Mater.* **13** 2105
[19] Li S Y, Lin P, Lee C Y, Tseng T Y and Huang C J 2004 *J. Phys. D: Appl. Phys.* **37** 1
[20] Jia H, Zhang Y, Chen X, Shu J, Luo X, Zhang Z and Yu D 2003 *Appl. Phys. Lett.* **82** 4146